



MICROSCOPIC AND CLUSTERING ANALYSIS OF KAOLIN BASED GEOPOLYMER LATERITICS SOIL. A CASE STUDY OF NORTH-CENTRAL NIGERIA

**Bamitale Dorcas Oluyemi-Ayibiowu¹, Lucia Omolayo Agashua¹
Igibah Christopher Ehizemhen^{2*}**

¹Department of Civil Engineering, Federal University of Technology Akure Ondo State, Nigeria

²Department of Civil Engineering, Federal University Oye-Ekiti, Ekiti State, Nigeria

*Corresponding Author

ABSTRACT

The strength of a fine-grained lateritic soil from three (3) different localities on Abuja – Lokoja road where road failure happen was treated with rice husk ash (RSA), cement and sodium silicate activator (SSA), with varying percentage examined by means of Atterberg, Compaction and triaxial shear tests. Conductivity has the highest mean (144.67mg/l) and followed by total dissolved solid (TDS) (94.00mg/l) while salinity recorded the lowest (0.06mg/l). Also, TDS recorded the highest Standard deviation (1.10mg/l).

KEYWORDS: *Geopolymer, Cluster, Construction, Sodium silicate, Abuja.*

1.0 INTRODUCTION

Majority of the road failures are normally reported as outcome of traffic overloading and environmental influences, distress investigations reveal that most of the road failures in Nigeria develop prematurely due to the use of substandard construction materials, poor construction techniques and soil conditions [1-3]. Subgrades are commonly compacted before the construction of a road [4-5], pavement or railway track [6], and are sometimes stabilized by the addition of asphalt, lime, portland cement or other modifiers [7-9]. The subgrade is the foundation of the pavement structure, on which the subbase is laid down. Laterites vary in color, but are usually brightly colored [10-13]. The shades most frequently encountered are pink, ochre, red and brown; however, some occurrences are mottled and streaked with violet, and others exhibit green marbling [14-17]. A single sample may exhibit a whole range of colors merging more or less perceptibly into one another in a variety of patterns and forms. Laterites owe their color to iron oxides in various states of hydration and sometimes also to manganese [18-20]. Their mineralogy generally involves quartz, kaolinite, hematite, goethite, and sometime maghemite. Kaolinite is always present with iron oxides [21-24]. The physical properties of lateritic soil vary according to the mineralogical composition and particle size distribution of the soil [25-27]. Stabilization technique has been a concern to transportation planners and designers for the past decade as alternatives to cut off or scrap unsuitable materials when encountered on site [28-30]. An alteration to the physical or engineering properties of a soil mass will require investigation of economic alternatives such as relocation of the site or use of borrowed materials [31-33]. At present, most of the desirable building sites near urban areas have been used making alternative location not practical. Geopolymer is a product of the alkali activation of aluminosilicate materials present in industrial waste materials such as furnace slag, slag furnace, granulated blast-furnace slag, fly ash, kaolin clay and red mud [34-38]. Geopolymer like ground granulated blast-furnace slag (an industrial waste produced from the cement production) and kaolin clay (natural occurring waste). Whereas rice husk fibre is waste from agricultural. Besides, globally, ground granulated blast-furnace slag and rice husk fiber produced by cement factories and rice industries have been increasing for the past few years. The mass production of both ground granulated blast-furnace slag and rice husk



fiber causes disposal problems and an increase in expenses for storage in available landfills. This eventually poses a threat to the environment if it is not properly managed. The use of geopolymeric materials in setting soil improvement is growing daily [39-42]. Unfortunately, little research has been completed to distinguish between products that deliver enhanced performance and those that do not [43-47]. The nature of soil stabilization dictates that products may provide soil-specific properties and/or provide compatibility with environment. In other words, some products may work well in specific soil types in a given environment but perform poorly when applied to dissimilar materials in a different environment [5-6,48-49]. The use of geopolymer materials as soils stabilizers has been widely studied and results of such past studies indicate that geopolymers could be used as an effective soil stabilizer.

2.0 LITERATURE REVIEW

2.1 Concept of water

Globally, it is expected that land and water resources will continue to develop, since majority of the surface water bodies like streams, rivers etc. interact with groundwater [50]. Some interactions include: discharge of groundwater (containing solutes) into surface water features and groundwater recharge by surface water bodies causes variations in groundwater quality. With a rapid population growth, urbanization, contamination and contributions from the air through the burning of biomass materials induce environmental deterioration, especially dangers on water supplies due to microbial and chemical pollutants will definitely rise [51-53]. Waste disposed at dumpsites, burning of waste materials and storm water runoff carry contaminants to nearest ground and surface water sources. Determining the concentration of pollutants (by comparing measured parameters with international standards) and evaluating the level of pollution of water supply are conducted to examine the impact of quality control measures on water quality.

2.2 Multivariate concept

The multivariate statistical analysis is a technique which deals with data that comprises of sets of measurements or a number of variables (individuals or objects) as observed [52]. Its analysis is to clearly reveal the governing processes through reduction and grouping of a given data. Multivariate approach is regarded as a very useful tool for dealing with the increasing number of parameters that affect water quality. They have been applied in many areas of research work, such as, surface water quality assessment [53-55]; to evaluate the parameters involved in surface-groundwater relationship (hydrogeochemical) as suggested [56] and [57]. Multivariate analysis can aid simplification and classification of large data sets and are also useful for drawing significant deductions as observed [58]. Factor and Cluster analyses are few of the common and efficient ways of showing complex relationships among many variables (objects) as stated by [56]. Among the multivariate statistical techniques, the hierarchical cluster analysis (HCA) and principal components analysis (PCA) are mainly used in water quality studies. In cluster analysis (CA), the data cluster is divided into groups in terms of the similarities and differences, and the dimensionality of a data cluster is degraded to a new variable group via the principal components analysis [52-54]. The systems monitor the time-based changes in water systems, and to obtain useful findings. application of different multivariate approaches (cluster analysis (CA), principal components analysis, source apportionment by multiple regression on principal components) for the interpretation of these complex data, matrices offers a better understanding of water quality and ecological status of the studied systems and allows the identification of the possible factors/sources that influence the water systems and offers a valuable tool for reliable management of water resources as well as rapid solutions on pollution problems [51,57].

2.3 Microstructure analysis

X-ray diffraction (XRD) is a nondestructive technique that provides detailed information about the crystallographic structure, chemical composition, and physical properties of materials [46-47]. XRD is a powerful nondestructive technique for characterizing crystalline materials. It provides information on structures, phases, preferred *crystal* orientations (texture), and other structural parameters, such as average grain size, crystallinity, strain, and *crystal* defects [48-49]. Scanning electron Microscopy (SEM) is a type of electron microscope that produces images of a sample by scanning the surface with a focused beam of electrons [46,48]. The electrons interact



with atoms in the sample, producing various signals that contain information about the surface topography and composition of the sample. The electron beam is scanned in a raster scan pattern, and the position of the beam is combined with the intensity of the detected signal to produce an image

3.0 ANALYSIS RESULTS

3.1 Descriptive Statistics

Table 1 and Figure 1 shows the result of the physical parameters of water utilized for geopolymer analysis. The result showed that Conductivity has the highest mean (144.67mg/l) and followed by total dissolved solid (TDS) (94.00mg/l) while salinity recorded the lowest (0.06mg/l). Also, TDS recorded the highest Standard deviation (1.10mg/l). This was followed by total suspended solid (TSS) (0.75mg/l) while salinity recorded the least value of (0.006mg/l). Thus, all the parameter of all the water samples examined are within the maximum permissible limit of Federal Ministry of works and Housing standards for construction water quality.

3.2 Cluster Analysis (Using Squared Euclidean distance)

Result from Table 2 which were graphically represented in Figures 2 & 3 detect similarity groups between the lateritic soils and geopolymer. Two statistically significant clusters are formed for Atterberg C1 and C2, which yielded two groups of similarity between the sampling sites. CBR, compaction, UCS and Triaxial test represented are presented as A and B. Temporal cluster analysis was used on standardized log-transformed data sorted by season. CA was performed using squared Euclidean distances as a measure of similarity.

3.3 Impact of Correlation Analysis (Atterberg limit, compaction, CBR and UCS)

The laboratory experimental results analysis for this research work was carried out using Correlation analysis as the primary statistical tool and statistical package for social science (SPSS) as statistical software packages for statistical analysis. Correlation analysis is a statistical technique to quantify the dependence of two or more variables. The purpose of a correlation analysis is to determine whether there is a relationship between sets of variables CBR, RHA, and OMC or UCS, RHA, and OMC and the Outcomes of correlation are summarized in Table 3 & 4 and Figure 4. Inference was based on the strength tests (CBR soaked and UCS) results gotten from cement, Rice Husk Ash (RHA), kaolin clay powder and geopolymer mix stabilized soil other than those obtained from RH. Each of the parameters pair were calculated using Pearson's correlation coefficients as displayed in Table 5. A significant correlation was found to exist between Geopolymer and Kaolin clay powder ($r = 0.95$, $\alpha = 0.05$).

3.3.1 Correlation analysis for unconfined compressive strength

Regression analysis predict the interaction between sets of variables (one or more) called independent variables and a single variable called dependent variable. Researches in sciences and engineering have applied regression analysis to buttress relationships between two variables or sets of variables [13-15]. The regression plot indicates that all the parameters considered have influence on the UCS values of stabilized soil. The coefficients of regression for each parameter would reveal the level of the effect of the parameter on the UCS. KCP, RHA and OMC have positive coefficients which depict the fact that increase in these parameters lead to improvement in UCS of the compacted soil Table 3. Similarly, the MDD, PF, PI and CE have negative coefficients, which depict decrease in UCS with increase in these variables. Care should be taken to ensure these variables are properly controlled at the site during field compaction to achieve a durable road pavement.

3.3.2 Correlation analysis for California bearing ratio

Regression analysis result for California bearing ratio are presented in Figure 4 and Table 4. Result of regression analysis show that all the parameters considered have effect on the CBR of the treated soil with correlation coefficient value of $R^2 = 92.7\%$. The coefficients of each parameter reveal the magnitude of the effect of the parameter on the CBR. MDD have positive coefficients which depict the fact that increase in these parameters will lead to improvement in CBR of the compacted soil. Similarly, the OMC, PF, PI and CE have negative coefficients, which depict decrease in CBR with increase in these variables.

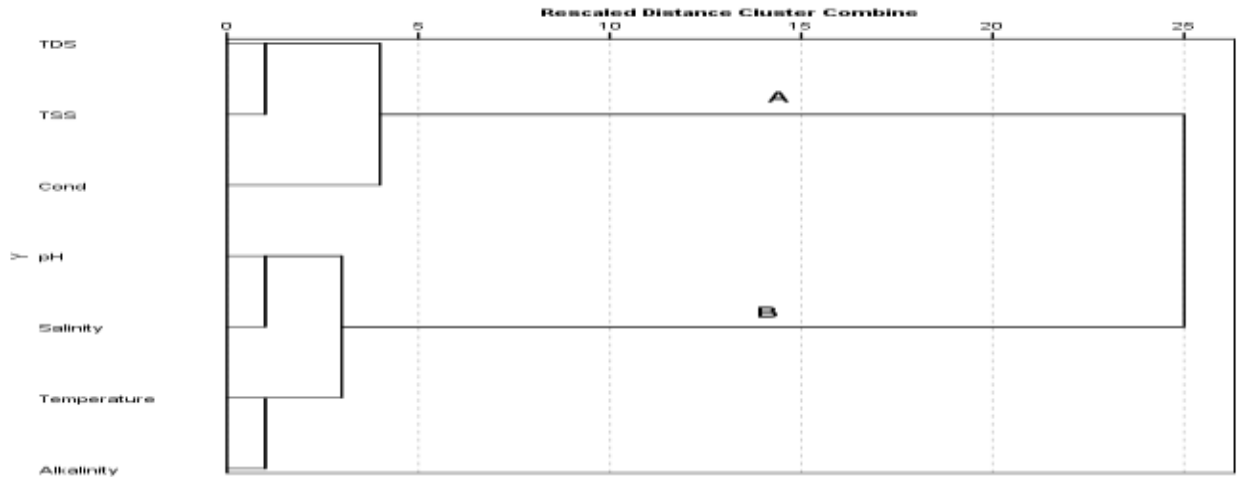


Figure 2: Dendrogram for water test.

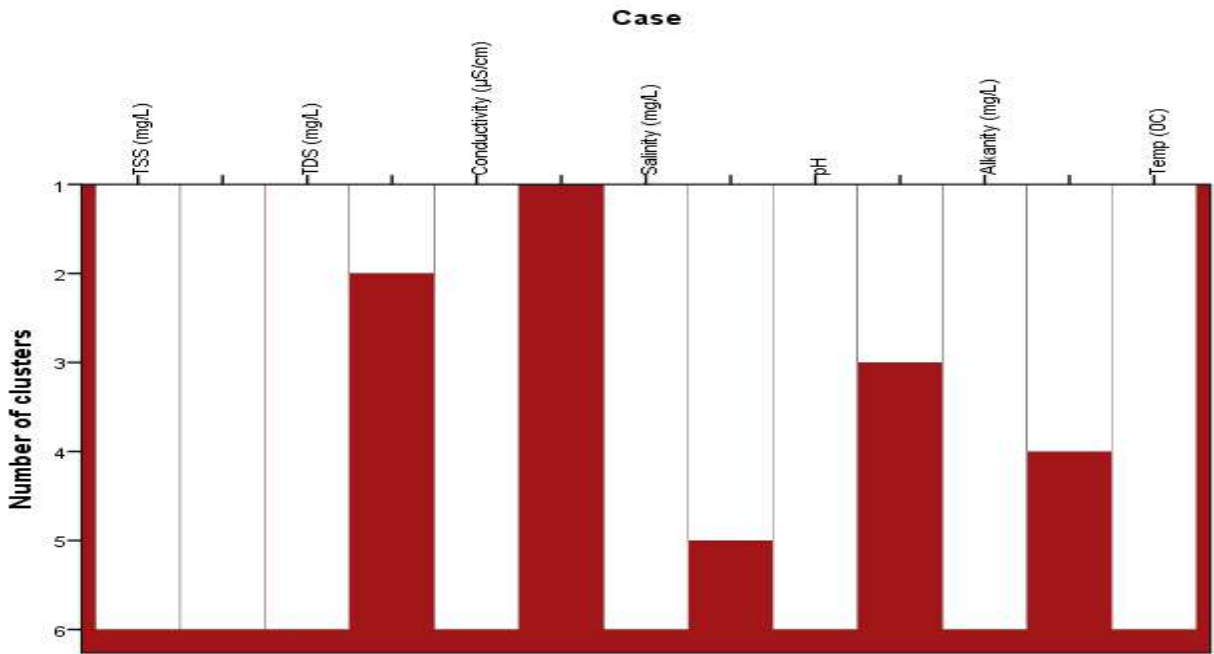


Figure 3: Numbers of clusters for water test



Table 2: Agglomeration schedule of Cluster Analysis (Water Test)

Stage	Cluster Combined		Coefficients	Stage Cluster First Appears		Next Stage
	Cluster 1	Cluster 2		Cluster 1	Cluster 2	
1	4	5	17.500	0	0	5
2	2	7	136.942	0	0	4
3	1	6	2199.817	0	0	4
4	1	2	10272.836	3	2	6
5	3	4	20986.002	0	1	6
6	1	3	101760.520	4	5	0

Table 3: Relationship between UCS, cement, RHA, KCP and OMC (H_1 : there is significant relationship between, CBR, OMC and geopolymers).

Variable	N	Mean	Std Dev	r-cal	P-value	Remark
Stabilizer	6	441.97	191.88	0.980	0.003	Reject H_0
Cement	6	64.06	21.63			
RHA	6	74.07	25.21			
KCP	6	358.20	145.04			

Table 4: Relationship between CBR, cement, RHA, KCP and OMC (H_0 : there is significant relationship between, CBR, OMC and geopolymers).

Variable	N	Mean	Std Dev	r-cal	P-value	Remark
Stabilizer	6	92.91	46.19	0.998	0.002	Reject H_0
Cement	6	32.73	14.25			
RHA	6	71.83	32.90			
KCP	6	76.65	37.29			

3.5 Effect on X-ray diffraction, XRF, SEM, EDAX and FTIR.

3.5.1 Effect on X-ray diffraction

The effect of addition of additives on the soil structure has been observed by X-ray diffraction test. Figure 5 shows the XRD patterns for natural and chemically treated laterite soil. XRD technique was used to achieve two goals: first, involving the measurement of mineralogical changes of soil structure due to the presence of liquid stabilizer, and secondly, to find newly formed crystalline cementitious compounds. A Bruker D8 advanced diffractometer was employed for the analysis of cured samples. The Cu-K α radiation ($k = 1.54 \text{ \AA}$) at an angle scan (2θ) of 6–90°, step size of 0.02°, and 1 s lodging at each step was used for scanning. The high resolution images of fabric of the soil prior and after the treatment were captured by a SEM that was equipped with EDAX. In order to prepare the samples, they were completely covered by platinum under highly vacuum environment. Moreover, the EDAX method was used to find the major elemental composition on the surface of treated particles. The results were presented based on the ratios of Al:Si and Na:Si at varying time intervals. The analysis of FTIR was applied on treated samples to determine their molecular structural changes. In order to measure the absorption bands of the prepared KBr disk, a 2 mg sample of grounded dried soil was mixed with 200 mg KBr. The sample was scanned by a Perkin Elmer Spectrum 2000 gadget in the 400–4,000 cm^{-1} infrared spectrum range [47]. A comparison was made between the resultant patterns and the standard dataset from Joint Committee for Powder Diffraction Standards [49]. This figure explains that the new structure soil has been appeared in soil stabilized with 4% cement, KCP and geopolymers, and 20% RHA. Presence of the analcite and carbonate at peak 3.43 and 3.30 A° exhibits a reaction processed. This implies that pozzolanic reaction is taking a place to form a cementitious material. The peak of quartz (3.34 A°) and feldspar (6.14 A°) has been disappeared at stabilized residual soil.

The main existed minerals in the laterite soil specimens were kaolinite and gibbsite [46–48]. Comparisons of the XRD results for the treated and untreated samples showed that quartz was unaffected by the treatment. However, there was a noticeable change in the XRD results for the kaolinite spectra. Generally, in all of the treated samples,



few peaks were diminished and reduced slightly. This was because of the stabilizer effect and its weathering action on the clay minerals. However, no new peaks due to the gel-form (amorphous) structure of formed reaction products were obtained [47-49].

3.5.2 Effect on XRF

The impact of addition of additives on the soil structure has been observed by X-ray fluorescent test. Figure 6 shows the XRF patterns for natural and chemically treated laterite soil. XRF (X-ray fluorescence) is a non-destructive analytical technique used to determine the elemental composition of materials. XRF analyzers determine the chemistry of a sample by measuring the fluorescent (or secondary) X-ray emitted from a sample when it is excited by a primary X-ray source.

3.5.3 Effect on SEM

Micro-analyses of the treated samples in the SEM were also performed at different time intervals. Figure 7 presents the SEM results of untreated and treated soil samples. The existence of free oxides within the untreated soil covered and bonded the soil particles together in a big packet fabric. On the other hand, the formation of new white layers of reaction products on the surface of lateritic soil particles samples is evident. These compounds were roughly identified as sodium aluminosilicate hydrate (N-A-S-H) [46-48].

3.5.4 Effect on FTIR

The FTIR analysis is used to measure the absorption bands at characteristic wavelengths of bonds that vibrate independently of one another in order to define the functional groups of soil minerals. Figure 8 shows the FTIR spectra for the natural and chemically stabilized samples. The common features of FTIR spectra involved the following: the bands at 1,111 and 1,028 cm^{-1} indicated the perpendicular and in-plane Si-O stretching, respectively. The peaks at 3,615 cm^{-1} corresponded to inner OH-stretching vibrations and band at 3,692 cm^{-1} was inner-surface hydroxyl groups [47]. The latter was a typical band of kaolinite mineral, while the former was a characteristic of various phyllosilicate minerals. Moreover, the band at 910 and 792 cm^{-1} indicated the existence of hematite, respectively [48,49]. The other bands including the Si-O vibrations observed at 535, and 466 cm^{-1} mostly defined the existence of kaolinite mineral. A stretching vibration was identified at 3,446 cm^{-1} , while the 1,637 cm^{-1} band was an H-O-H flexible band of water with an overtone happening at 3,378 cm^{-1} . The results of FTIR spectrum for 7, and 14 days cured samples confirmed that the chemical treatment was able to make a noticeable difference in the Si-O functional groups of soil particles. Also, in general the peaks intensities reduced with curing time. This was because of the weathering action of the stabilizer on the clay minerals [46-49].

CONCLUSION

Two statistically significant clusters are formed A and B, which yielded two groups of similarity between the three lateritic soil and the geopolymer materials. The statistical analysis for CBR and UCS shows a positive correlation (between the CBR, RHA and the OMC which indicate a direct relationship between the variables). A significant correlation was found to exist between Geopolymer and Kaolin clay powder ($r = 0.95$, $\alpha = 0.05$). Also, it was found that for the samples treated with higher liquid stabilizer content (more than 8 % SSA) a lower compressive strength was achieved. The latter was probably due to the increase in the positive surcharge and the subsequent repulsion of soil particles inside the mixture. Hence, 8 % of SSA was chosen as the optimum value that was added to the laterite soil for micro-structural studies. Based on the SEM and EDAX results the new formed gel-like cementitious compounds of sodium aluminosilicate hydrate (N-A-S-H) were believed to be the main cause of strength development. The XRD results also revealed a general increase in the lateritic soil mineral peaks.



REFERENCES

1. E. Adeyanju, C. Okeke. (2019). Exposure effect to cement dust pollution : a mini review , *SN Appl. Sci.* 1. 1–17. <https://doi.org/10.1007/s42452-019-1583-0>.
2. N. Wen, Y. Zhao, Z. Yu, M. Liu, A sludge and modified rice husk ash-based geopolymer: synthesis and characterization analysis, *J. Clean. Prod.* 226 (2019) 805–814. <https://doi.org/10.1016/j.jclepro.2019.04.045>.
3. A.A. Alshaba, T.M. Abdelaziz, A.M. Ragheb (2018). Treatment of collapsible soils by mixing with ironpowder. 3737–3745. <https://doi.org/10.1016/j.aej.2018.07.019>.
4. M.A. Rahgozar, M. Saberian, J. Li, Soil stabilization with non-conventional eco-friendly agricultural waste materials: An experimental study, *Transp. Geotech.* 14 (2018) 52–60. <https://doi.org/10.1016/j.trgeo.2017.09.004>.
5. N. Yoobanpot, P. Jamsawang, K. Krairan, P. Jongpradist, S. Horpibulsuk, Reuse of dredged sediments as pavement materials by cement kiln dust and lime treatment, *Geomech. Eng.* 15 (2018) 1005–1016. <https://doi.org/10.12989/gae.2018.15.4.1005>.
6. Roychand R. Development of zero cement composite for the protection of concrete sewage pipes from corrosion and fatbergs. *ResourConservRecycl* 2021; 164:105166.
7. Igibah C, Agashua L and Sadiq A (2020). Influence of hydrated lime and bitumen on different lateritic soil samples: Case study of Sheda-Abuja, Nigeria. *IJET*, 1-7.
8. Pooria G, Mostafa Z, Nazanin M, Mohammad S, Jie L, Navid R. Shear strength and life cycle assessment of volcanic ash-based geopolymer and cement stabilized soil: A comparative study. *Transportation Geotechnics* 31 (2021) 100639
9. Xu Zifang, Ye Dongdong, Dai Tao & Dai Yan (2021) Research on Preparation of Coal Waste-Based Geopolymer and Its Stabilization/Solidification of Heavy Metals, *Integrated Ferroelectrics*, 217:1, 214-224, DOI: 10.1080/10584587.2021.1911314
10. Abdullah H. Cyclic behaviour of clay stabilised with fly-ash based geopolymer incorporating ground granulated slag. *TranspGeotech* 2021;26: 100430.
11. Upshaw M and Cai C. S (2021). Feasibility study of MK-based geopolymer binder for RAC applications: Effects of silica fume and added CaO on compressive strength of mortar samples. *Case Studies in Construction Materials* Volume 14, e00500
12. Adeyanju Emmanuel, OkekeChukwueloka Austin, Akinwumi Isaac and BusariAyobami (2020). Subgrade stabilization using Rice Husk Ash-Geopolymer (GPHA) and Cement Klin Dust (CKD).
13. Wang, S.; Xue, Q.; Zhu, Y.; Li, G.; Wu, Z.; Zhao, K. Experimental study on material ratio and strength performance of geopolymer improved soil. *Constr. Build. Mater.* **2020**, *267*, 120469. [CrossRef]
14. Abdullah, H.H.; Shahin, M.A.; Walske, M.L. Review of Fly-Ash-Based Geopolymers for Soil Stabilisation with Special Reference to Clay. *Geosciences* **2020**, *10*, 249. [CrossRef]
15. Rivera, J.F.; Orobio, A.; Mejía De Gutiérrez, R.; Cristelo, N. Clayey soil stabilization using alkali-activated cementitious materials. *Mater. Construcción* **2020**, *70*, 211. [CrossRef]
16. Zhu, Y.; Chen, R.; Lai, H. Stabilizing Soft Ground Using Geopolymer: An Experimental Study. In *Proceedings of the CICTP 2020, Xi'an, China, 14–16 August 2020*; American Society of Civil Engineers (ASCE): Reston, VA, USA; pp. 1144–1155.
17. Agashua Lucia O and OgbiyeAdebanji S (2018). Influence of Cement, Bitumen and Lime on Some Lateritic Soil Samples as Pavement Material. *IOP Conf. Series: Materials Science and Engineering* 413 (2018) 012012 [doi:10.1088/1757-899X/413/1/012012](https://doi.org/10.1088/1757-899X/413/1/012012).
18. Agashua Lucia O, IgibahEhizemhen C and Sadiq, Abubakar. (2018). The Impact of Bituminous additive on Lateritic Soil with Varying Percentage for long lasting soil stabilizer.
19. A. Alhmed, N. Nagy, E.N. Naggar, T. Kamei, Stabilisation of soft soil with recycled plaster admixtures., in: *Proc. Inst. Civ. Eng. - Gr. Improv.*, 2018; pp. 1–9. <https://doi.org/doi.org/10.1680/jgrim.16.00038>.
20. Dheyab, W.; Ismael, Z.T.; Hussein, M.A.; Huat, B.B.K. Soil Stabilization with geopolymers for low cost and environmentally friendly construction. *Int. J. Geomate* **2019**, *17*, 271–280. [CrossRef]
21. Rivera J. Fly ash-based geopolymer as A4 type soil stabiliser. *TranspGeotech* **2020**; *25*:100409.
22. Seyhan F, Sedef D, Gülğün Y and Jamal M. (2020). Characteristics of Engineered Waste Materials Used for Road Subbase Layers. *KSCCE*.
23. Adeyanju Emmanuel, OkekeChukwueloka Austin, Akinwumi Isaac and BusariAyobami (2020). Subgrade stabilization using Rice Husk Ash-Geopolymer (GPHA) and Cement Klin Dust (CKD).
24. Farhangi V, Karakouzian M, Geertsema M. Effect of micropiles on clean sand liquefaction risk based on CPT and SPT. *ApplSci* **2020**; *10*(9):3111.
25. Saberian M, et al. Application of demolition wastes mixed with crushed glass and crumb rubber in pavement base/subbase. *ResourConservRecycl* **2020**; *156*: 104722.



26. RezazadehEidgahee D, Rafiean AH, Haddad A. A novel formulation for the compressive strength of IBP-based geopolymer stabilized clayey soils using ANN and GMDH-NN approaches. *Iranian J SciTechnol, Trans Civil Eng* 2020;44(1): 219–29. MolaAbasi H, et al. Evaluation of the long-term performance of stabilized sandy soil using binary mixtures: A micro-and macro-level approach. *J Cleaner Prod* 2020:122209.
27. Abdullah, H.H.; Shahin, M.A.; Walske, M.L.; Karrech, A. Systematic approach to assessing the applicability of fly-ash-based geopolymer for clay stabilization. *Can. Geotech. J.* **2020**, *57*, 1356–1368. [CrossRef]
28. Khasib, I.A.; Daud, N.N.N. Physical and Mechanical Study of Palm Oil Fuel Ash (POFA) based Geopolymer as a Stabilizer for Soft Soil. *Pertanika J. Sci. Technol.* **2020**, *28*, 149–160. [CrossRef]
29. Ghadakpour M, Choobasti AJ, Kutanaei SS. Experimental study of impact of cement treatment on the shear behavior of loess and clay. *Arabian J Geosci* 2020; 13(4):184.
30. Abdulkareem M, et al. Environmental and economic perspective of waste-derived activators on alkali-activated mortars. *J Cleaner Prod* 2020;280:124651.
31. Vitale, E.; Russo, G.; Deneele, D. Use of Alkali-Activated Fly Ashes for Soil Treatment. In *Geotechnical Research for Land Protection and Development*; Calvetti, F., Cotecchia, F., Galli, A., Jommi, C., Eds.; Lecture Notes in Civil Engineering; Springer International Publishing: Cham, Switzerland, 2020; Volume 40, pp. 723–733. ISBN 978-3-030-21358-9.
32. Abdullah, H.H.; Shahin, M.A.; Walske, M.L. Geo-mechanical behavior of clay soils stabilized at ambient temperature with fly-ash geopolymer-incorporated granulated slag. *Soils Found.* **2019**, *59*, 1906–1920. [CrossRef]
33. Yaghoubi M, Arulrajah A, Disfani MM, Horpibulsuk S, Darmawan S, Wang J. Impact of field conditions on the strength development of a geopolymer stabilized marine clay. *Appl Clay Sci* 2019;167:33–42.
34. Jahandari S, Saberian M, Zivari F, Li J, Ghasemi M, Vali R. Experimental study of the effects of curing time on geotechnical properties of stabilized clay with lime and geogrid. *Int J GeotechEng* 2019;13(2):172–83.
35. N. Wen, Y. Zhao, Z. Yu, M. Liu, A sludge and modified rice husk ash-based geopolymer: synthesis and characterization analysis, *J. Clean. Prod.* 226 (2019) 805–814.
36. <https://doi.org/10.1016/j.jclepro.2019.04.045>.
37. Amiri E, Emami H. Shear strength of an unsaturated loam soil as affected by vetiver and polyacrylamide. *Soil Tillage Res* 2019;194:104331.
38. Chang Ilhan, Cho Gye-Chun. Shear strength behavior and parameters of microbial gellan gum-treated soils: from sand to clay. *ActaGeotech* 2019;14(2):361–75.
39. Elandaloussi R, et al. Effectiveness of lime treatment of coarse soils against internal erosion. *GeotechGeolEng*, 2019. 37(1): p. 139-154.
40. Pradhan Subhasis, Tiwari BR, Kumar Shailendra, BaraiSudhirkumar V. Comparative LCA of recycled and natural aggregate concrete using Particle Packing Method and conventional method of design mix. *J Cleaner Prod* 2019;228: 679–91.
41. D. Kuang et al. , Influence of angularity and roughness of coarse aggregates on asphalt mixture performance. *Constr Build Mater.* **200** , 681 (2019). DOI: 10.1016/j.conbuildmat.2018.12.176. [Crossref], [Web of Science ®], [Google Scholar]
42. E.A. Adeyanju, C.A. Okeke. (2019a) Clay soil stabilization using cement kiln dust, in: *IOP Conf. Ser. Mater. Sci. Eng.* pp. 1–10.
43. E. Adeyanju, C. Okeke. (2019b). Exposure effect to cement dust pollution : a mini review , *SN Appl. Sci.* *1*. 1–17. <https://doi.org/10.1007/s42452-019-1583-0>.
44. A.A. Alshaba, T.M. Abdelaziz, A.M. Ragheb (2018). Treatment of collapsible soils by mixing with ironpowder. 3737–3745. <https://doi.org/10.1016/j.aej.2018.07.019>.
45. N. Wen, Y. Zhao, Z. Yu, M. Liu, A sludge and modified rice husk ash-based geopolymer: synthesis and characterization analysis, *J. Clean. Prod.* 226 (2019) 805–814. <https://doi.org/10.1016/j.jclepro.2019.04.045>.
46. Cong, P., Cheng, Y., (2021). Advances in geopolymer materials: A comprehensive review, *Journal of Traffic and Transportation Engineering (English Edition)*, <https://doi.org/10.1016/j.jtte.2021.03.004>.
47. Zhao, S., Xia, M., Yu, L., et al., 2021. Optimization for the preparation of composite geopolymer using response surface methodology and its application in lead-zinc tailings solidification.
48. Pelisser, F., Bernardin, A.M., Michel, M.D., et al., 2021. Compressive strength, modulus of elasticity and hardness of geopolymeric cement synthesized from non-calcined natural kaolin. *Journal of Cleaner Production* 280 (part 1), 124293.
49. Rosyidi, S.A.P., Rahmad, S., Yusoff, N.I.M., et al., 2020. Investigation of the chemical, strength, adhesion and morphological properties of fly ash based geopolymermodified bitumen. *Construction and Building Materials* 255, 119364.



50. Achieng A, P. Raburu, EKipkorir, SNgodhe, KObiero, J Ani-Sabwa. "Assessment of water quality using multivariate techniques in River Sosiani, Kenya" *Environmental Monitoring and Assessment*, vol 189, pp 28-37, June 2017.
51. Aghazadeh, N., Chitsazan, M., &Golestan, Y. (2016). Hydrochemistry and quality assessment of groundwater in the Ardabil area, Iran. *Applied Water Science*, 7(7), 3599– 3616. <https://doi.org/10.1007/s13201-016-0498-9>.
52. Ahmed F, A. N. M. Fakhruddin, T. M. D. Imam, N. Khan, T. A. Khan, M. M. Rahman, A. T. M. Abdullah, "Spatial Distribution and Source Identification of Heavy Metal Pollution in Roadside Surface Soil: A Study of Dhaka Aricha Highway, Bangladesh," *Ecol Process* 5:2, 2016.
53. Barzegar, R., AsghariMoghaddam, A., &Tziritis, E. (2017). Hydrogeochemical
54. features of groundwater resources in Tabriz plain, northwest of Iran. *Applied Water Science*, 7, 3997–4011. <https://doi.org/10.1007/s13201-017-0550-4>.
55. Bhardwaj R, A. Gupta, J. K. Garg, "Evaluation of Heavy Metal Contamination Using Environmetrics Andindexing Approach for River Yamuna, Delhi stretch, India," *Water Science* 31, pp. 52–66, 2017.
56. Bhardwaj R, A. Gupta, J. K. Garg, "Evaluation of Heavy Metal Contamination Using EnvironmetricsAndindexing Approach for River Yamuna, Delhi stretch, India," *Water Science* 31, pp. 52–66, 2017.
57. Bodrud-Doza, A.R.M. Towfiqul Islam, F. Ahmed, S. Das, N. Saha, S. M. Rahman, "Characterization of Groundwater Quality Using Water Evaluation Indices, Multivariate Statistics and Geostatistics in Central Bangladesh," *Water Science* 30, pp. 19–40, 2016.
58. Bora, M., &Goswami, D. C. (2016). Water quality assessment in terms of water quality index (WQI): case study of the Kolong River, Assam, India. *Applied Water Science*, 7(6), 3125– 3135. <https://doi.org/10.1007/s13201-016-0451-y>.



APPENDIX

Table 1: Descriptive analysis (Water test)

		Temp (0C)	pH	Conductivity (µS/cm)	TDS (mg/L)	TSS (mg/L)	Alkanity (mg/L)	Salinity (mg/L)
N	Valid	6	6	6	6	6	6	6
	Missing	1	1	1	1	1	1	1
Mean		26.7833	6.3667	144.6667	94.0000	91.8333	53.0000	.0570
Std. Deviation		.11690	.05164	.51640	1.09545	.75277	.63246	.00063
Variance		.014	.003	.267	1.200	.567	.400	.000
Skewness		-.668	-.968	-.968	-1.369	.313	.000	.000
Std. Error of Skewness		.845	.845	.845	.845	.845	.845	.845
Kurtosis		-.446	-1.875	-1.875	2.500	-.104	2.500	2.500
Std. Error of Kurtosis		1.741	1.741	1.741	1.741	1.741	1.741	1.741
Range		.30	.10	1.00	3.00	2.00	2.00	.00
Minimum		26.60	6.30	144.00	92.00	91.00	52.00	.06
Maximum		26.90	6.40	145.00	95.00	93.00	54.00	.06

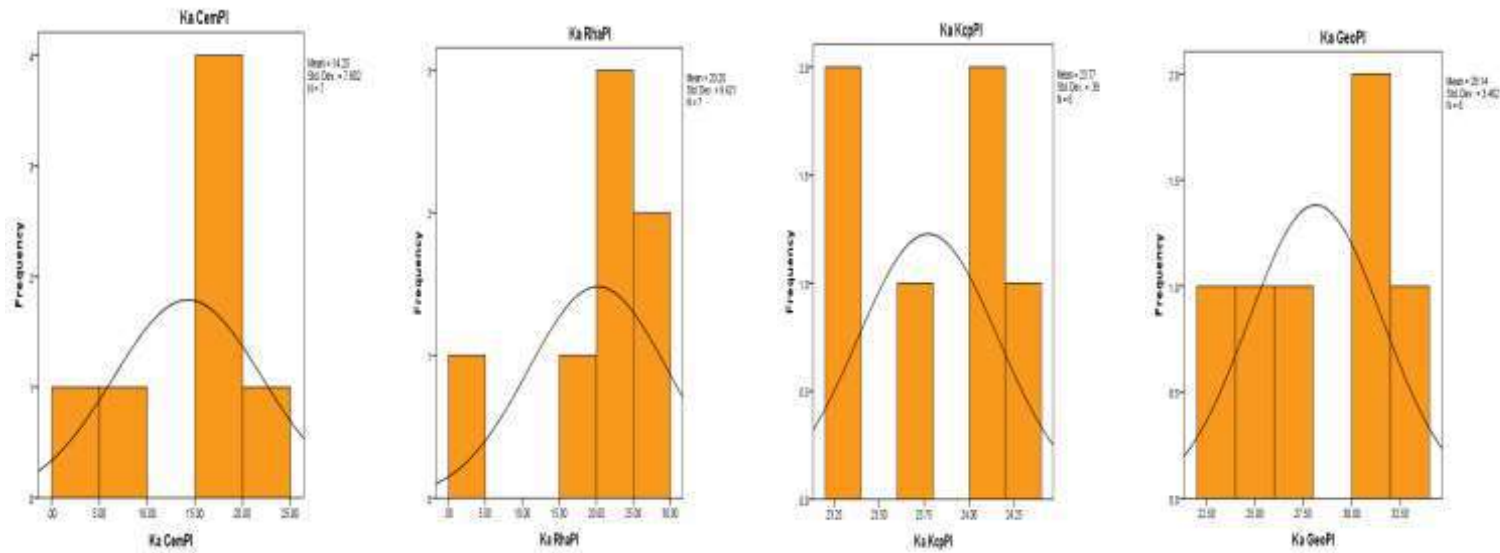


Figure 1: Histogram plot for cement, RHA, KCP and geopolymer stabilized soil.



Table 5: Correlation analysis for Atterberg test (1- tailed significant)

		Correlations												
		percent	Ka CemPI	Sa CemPI	Da CemPI	Ka RhaPI	Sa RhaPI	Da RhaPI	Ka KcpPI	Sa KcpPI	Da KcpPI	Ka GeoPI	Sa GeoPI	Da GeoPI
Pearson Correlation	percent	1.000	-.714	-.416	-.729	.774	.962	.733	.859	-.788	.569	.845	.871	.795
	Ka CemPI	-.714	1.000	.866	.987	-.367	-.507	-.191	-.356	.710	-.880	-.696	-.712	-.533
	Sa CemPI	-.416	.866	1.000	.898	.117	-.173	.279	-.087	.730	-.643	-.485	-.618	-.123
	Da CemPI	-.729	.987	.898	1.000	-.320	-.519	-.151	-.361	.785	-.835	-.742	-.784	-.530
	Ka RhaPI	.774	-.367	.117	-.320	1.000	.845	.954	.723	-.221	.505	.532	.404	.886
	Sa RhaPI	.962	-.507	-.173	-.519	.845	1.000	.851	.942	-.672	.397	.732	.762	.775
	Da RhaPI	.733	-.191	.279	-.151	.954	.851	1.000	.786	-.207	.255	.517	.393	.783
	Ka KcpPI	.859	-.356	-.087	-.361	.723	.942	.786	1.000	-.641	.180	.540	.648	.531
	Sa KcpPI	-.788	.710	.730	.785	-.221	-.672	-.207	-.641	1.000	-.356	-.766	-.945	-.357
	Da KcpPI	.569	-.880	-.643	-.835	.505	.397	.255	.180	-.356	1.000	.502	.422	.659
	Ka GeoPI	.845	-.696	-.485	-.742	.532	.732	.517	.540	-.766	.502	1.000	.929	.749
	Sa GeoPI	.871	-.712	-.618	-.784	.404	.762	.393	.648	-.945	.422	.929	1.000	.591
	Da GeoPI	.795	-.533	-.123	-.530	.886	.775	.783	.531	-.357	.659	.749	.591	1.000
Sig. (1- tailed)	percent		.056	.206	.050	.036	.001	.049	.014	.031	.119	.017	.012	.029
	Ka CemPI	.056		.013	.000	.237	.152	.359	.244	.057	.010	.062	.056	.138
	Sa CemPI	.206	.013		.008	.412	.371	.296	.435	.050	.084	.165	.096	.408
	Da CemPI	.050	.000	.008		.268	.146	.387	.241	.032	.019	.046	.032	.139
	Ka RhaPI	.036	.237	.412	.268		.017	.002	.052	.337	.153	.139	.213	.009
	Sa RhaPI	.001	.152	.371	.146	.017		.016	.002	.072	.218	.049	.039	.035
	Da RhaPI	.049	.359	.296	.387	.002	.016		.032	.347	.313	.147	.220	.033
	Ka KcpPI	.014	.244	.435	.241	.052	.002	.032		.085	.367	.135	.082	.139
	Sa KcpPI	.031	.057	.050	.032	.337	.072	.347	.085		.245	.038	.002	.243
	Da KcpPI	.119	.010	.084	.019	.153	.218	.313	.367	.245		.155	.202	.077
	Ka GeoPI	.017	.062	.165	.046	.139	.049	.147	.135	.038	.155		.004	.043
	Sa GeoPI	.012	.056	.096	.032	.213	.039	.220	.082	.002	.202	.004		.108
	Da GeoPI	.029	.138	.408	.139	.009	.035	.033	.139	.243	.077	.043	.108	
N	percent	6	6	6	6	6	6	6	6	6	6	6	6	6
	Ka CemPI	6	6	6	6	6	6	6	6	6	6	6	6	6
	Sa CemPI	6	6	6	6	6	6	6	6	6	6	6	6	6
	Da CemPI	6	6	6	6	6	6	6	6	6	6	6	6	6
	Ka RhaPI	6	6	6	6	6	6	6	6	6	6	6	6	6
	Sa RhaPI	6	6	6	6	6	6	6	6	6	6	6	6	6
	Da RhaPI	6	6	6	6	6	6	6	6	6	6	6	6	6
	Ka KcpPI	6	6	6	6	6	6	6	6	6	6	6	6	6
	Sa KcpPI	6	6	6	6	6	6	6	6	6	6	6	6	6
	Da KcpPI	6	6	6	6	6	6	6	6	6	6	6	6	6
	Ka GeoPI	6	6	6	6	6	6	6	6	6	6	6	6	6
	Sa GeoPI	6	6	6	6	6	6	6	6	6	6	6	6	6
	Da GeoPI	6	6	6	6	6	6	6	6	6	6	6	6	6

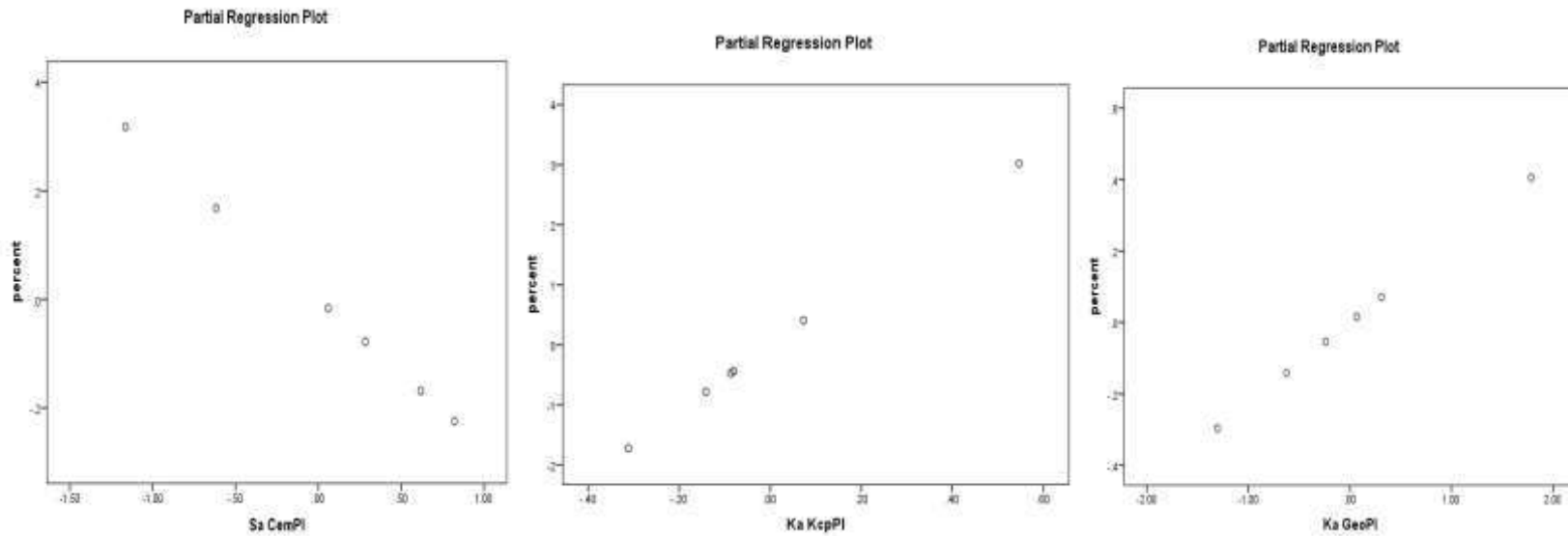


Figure 4: Correlation/ Regression Scatter plot from Atterbergtest results for cement, KCP and geopolymer for stabilized.



Da_20210611_103517_G04_S04_M04-Evaluation report (Da_20210611_103517_G04_S04_M04)

General information

Analysis date	2021-06-15 12:18:33	Measurement start time	2021-06-11 10:47:51
Analyst	Administrator	Operator	Administrator
Sample name	Da	Comment	
Measured data name	C:\WallPaper\11-06-2021\Da_20210611_103...	Memo	

Qualitative Analysis Results

Phase name	Formula	Figure of merit	Phase ref. detail	Space Group	DB Card Number
Quartz, syn	SiO2	0.952	S:\MPDF-4 Minerals 2020 R... 154; P321		01-077-8621
Muscovite	H2K Al3 (SiO4)3	3.289	S:\MPDF-4 Minerals 2020 R... 15; C12/c1		00-001-1090
Vermiculite	22MgO 5Al2O3 Fe2O3 ...	2.963	S:\MPDF-4 Minerals 2020 R... 15; C12/c1		00-002-9021
Chlorite (M)	Mg-SiO2-OH	2.944	S:\MPDF-4 Minerals 2020 R...		00-002-9025
Garnet	3(Ca, Fe, Mg)O (Al, Fe)...	2.978	S:\MPDF-4 Minerals 2020 R... 230; Ia-3d		00-002-0981
Sodalite	Na4Al3Cl3S6O12	1.506	S:\MPDF-4 Minerals 2020 R... 218; P-43n		00-003-4538

Path: C:\WallPaper\11-06-2021\Da_Solution.mxd Solution

Plot of results

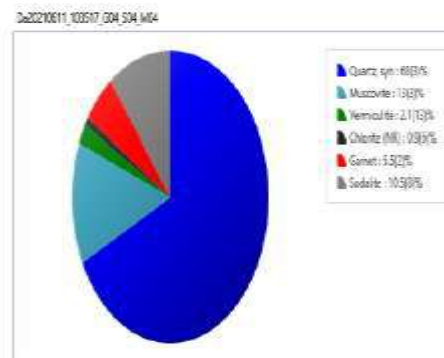


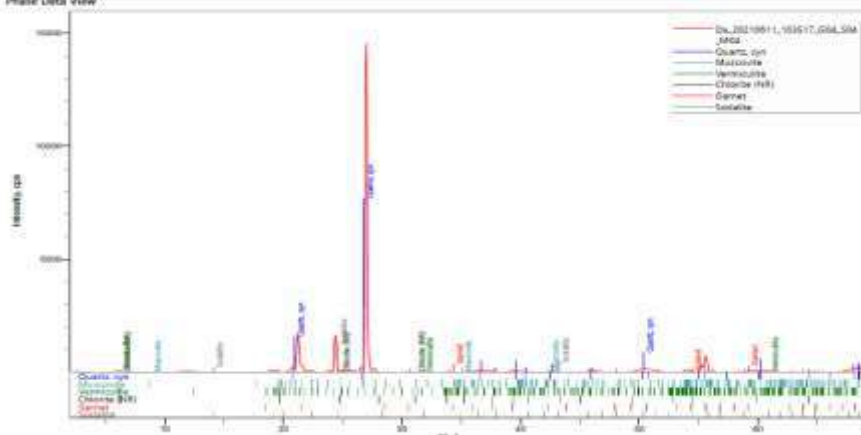
Table of results

Dataset / Weight Fraction	Value	Unit	Quartz, syn	Muscovite	Vermiculite	Chlorite (M)	Garnet	Sodalite
Da_20210611_103517_G04...	0		69.0	13.0	2.113	0.895	5.520	10.538

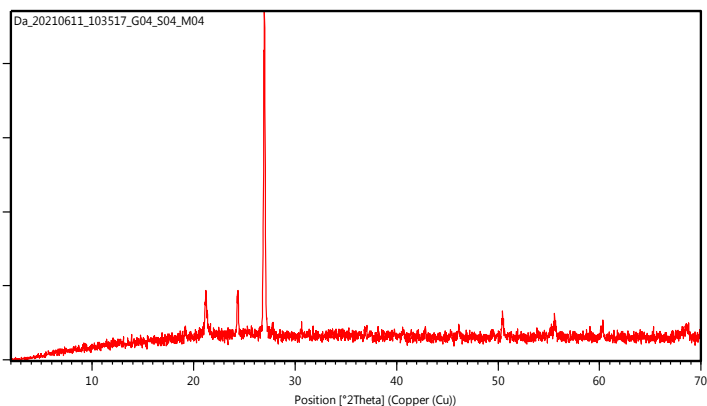
(a)

Path: C:\WallPaper\11-06-2021\Da_Solution.mxd Solution

Phase Data View



Counts



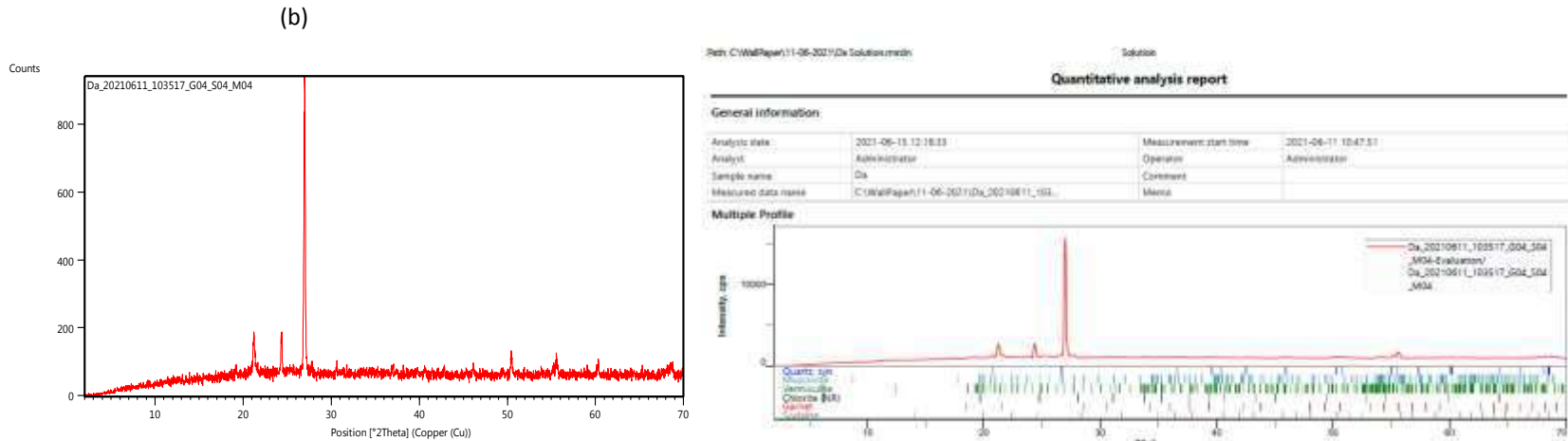


Figure 5: XRD analysis outcome on geopolymer lateritic soils.

Sample Name	DA		
Supplier	CLIENT		
Operator			
Date	6/11/2021 11:05		
GPS			
Testing time	15s		
Volt	45kV		
Curr	50uA		
Mode	Mineral Mode		
Specification			
Element	Content	Detection limit	Error
Al2O3 (%)	24.2641	0.0000	0.5581
SiO2 (%)	71.4911	0.0000	0.5350
K2O (%)	0.7214	0.0000	0.0776
TiO2 (%)	0.2449	0.0000	0.0132
MnO (%)	0.0142	0.0000	0.0012
Fe2O3 (%)	3.2110	0.0000	0.0244
Nb2O5 (%)	0.0103	0.0000	0.0001
Ag2O (%)	0.0024	0.0000	0.0001
CdO (%)	0.0215	0.0000	0.0010
Sb2O5 (%)	0.0189	0.0000	0.0010
PbO (%)	0.0003	0.0000	0.0000

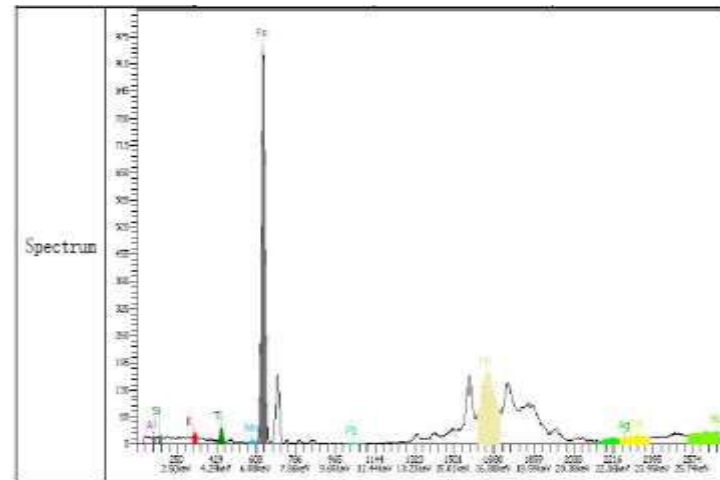


Figure6: XRF analysis outcome on geopolymers lateritic soils.

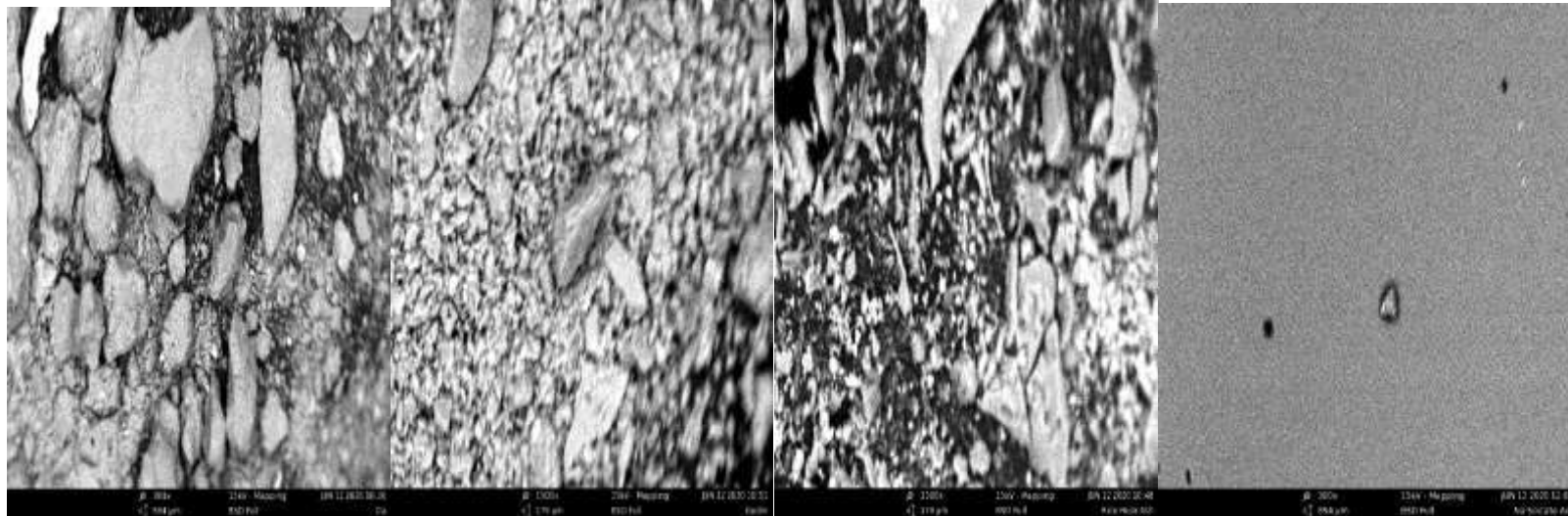


Fig. Figure 7: SEM for laterite, Kaolin, rice husk ash and Sodium silicate activator.

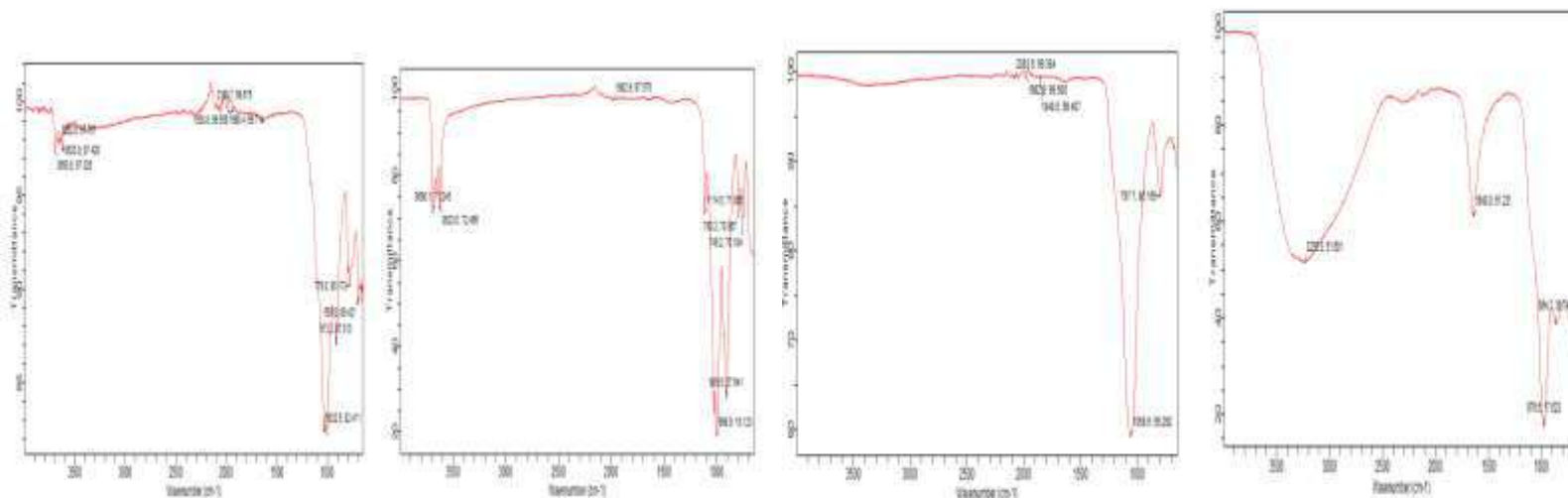


Figure 8: FTIR Spectrophor for laterite, kaolin, Rice Husk ash and Sodium silicate.